The Astrophysical Journal, 637:786–790, 2006 February 1

VOYAGER 1, *VOYAGER 2*, AND *PIONEER 10* Lyα DATA AND THEIR INTERPRETATION

P. Gangopadhyay,[1] V. V. Izmodenov,[2] M. Gruntman,[3] and D. L. Judge[1]

Received 2005 July 5; accepted 2005 September 30

ABSTRACT

The *Voyager 1* (*V1*), *Voyager 2* (*V2*), and *Pioneer 10* (*P10*) Lyα data sets are three of several diagnostic data sets available for the study of the very local interstellar medium (VLISM). Selected *V1* data obtained on 1989 day 279 at heliocentric distance of 39.1 AU in the upstream direction relative to the incoming interstellar neutral hydrogen flow and *V2* data obtained on 1990 day 143 at heliocentric distance of 32 AU, also in the upstream direction, have been used to estimate the local interstellar neutral hydrogen and proton densities and compared with *P10* data obtained in 1981 at distances between 23.39 and 23.87 AU in the downstream direction, respectively. State-of-the-art plasma-neutral and radiative transfer models have been used in the interpretation of the data. It has been found that a VLISM heliospheric model with neutral hydrogen density of 0.18 cm^{-3} and proton density of 0.06 cm^{-3} best fits both the *V1* data and the *V2* data. The *P10* data are best fitted by a VLISM model with neutral hydrogen density of 0.15 cm^{-3} and proton density of 0.05 cm^{-3}. The failure to find a single best-fit stationary heliosphere plasma-neutral model suggests, among other possibilities, that a quantitative interpretation of the heliospheric Lyα glow would require the incorporation of magnetic field and time dependence in the heliospheric model.

Subject headings: ISM: general — ultraviolet: ISM

Online material: color figures

1. INTRODUCTION

The heliosphere surrounding our Sun is a very complicated region that is shaped by the solar wind, the interstellar plasma, interstellar neutrals, magnetic field, and cosmic rays (Axford 1972; Holzer 1972; Zank 1999; Fahr 2004; Izmodenov 2004). The heliosphere provides a unique opportunity to study in detail the only accessible example of a commonplace but fundamental astrophysical phenomenon—the formation of an astrosphere. The heliospheric interface is a natural "environment" of our star, and the knowledge of its characteristics is important for the interpretation and the planning of space experiments.

Remote sensing of the VLISM using deep-space spacecraft EUV data is possible since the VLISM neutral hydrogen atoms, which scatter the solar Lyα photons, penetrate deeply into the heliosphere, although VLISM hydrogen atoms have a strong coupling with the heliospheric plasma protons. The distribution of these atoms inside the heliosphere is influenced by its journey through the interface between the heliosphere and the VLISM. Thus, interstellar hydrogen atoms provide excellent remote diagnostics on the structure of the heliospheric interface.

A quantitative study of the neutral hydrogen atom and proton density in the outer heliosphere has been made possible by the presence of four deep-space spacecraft, *P10*, *Pioneer 11* (*P11*), *V1*, and *V2*. The photometers on board *P10* and P11 and the ultraviolet spectrometers (UVSs) on board *V1* and *V2* have measured the interplanetary Lyα background radiation for more than 20 years. We present our study of *V1*, *V2*, and *P10* data. We have previously selected multiple spacecraft data spread over many years (Gangopadhyay et al. 2002, 2004; Izmodenov et al. 2003). We have in this work used a different selection procedure and chosen *V1* and *V2* data for one day and *P10* data for early 1981. The different data selection procedure was chosen to check whether a single stationary heliospheric model can fit multiple spacecraft data. This analysis uses the latest state-of-the-art neutral hydrogen plasma and radiative transfer models outlined in the following sections. The new results are presented and the implications discussed.

2. H ATOM DISTRIBUTION MODEL

The interaction of the solar wind with the interstellar medium influences the distribution of interstellar neutral atoms inside the heliosphere. The main difficulty in the modeling of the H atom flow in the heliosphere is its kinetic character due to the large (i.e., comparable to the size of the heliosphere) mean free path due to the charge-exchange reaction. In this paper we use the self-consistent model developed by Baranov & Malama (1993) to get the H atom distribution in the heliosphere and heliospheric interface structure. The kinetic equation for the neutral component and the hydrodynamic Euler equations were solved self-consistently by the method of global interactions. An advanced Monte Carlo method with splitting of trajectories (Malama 1991) was used to solve the kinetic equation for H atoms. Basic results of the model were reported by Baranov & Malama (1995), Izmodenov et al. (1999, 2001), and Izmodenov (2000, 2003, 2004).

3. RADIATIVE TRANSFER MODEL

A Monte Carlo radiative transfer code (Gangopadhyay et al. 1989, 2002) that includes a self-reversed solar line, multiple scattering, angle-dependent partial frequency redistribution, varying hydrogen density and temperature, and Doppler effect has been used. A full multiple scattering treatment is necessary to interpret the backscattered heliospheric Lyα data since the LISM neutral hydrogen gas is an optically thick medium for solar Lyα photons.

4. INSTRUMENTATION AND DATA

The UVSs on board *V1* and *V2* obtain spectra in the 500–1700 Å range. The UVS instrument is described in detail by

[1] Department of Physics, Astronomy and Space Sciences Center, University of Southern California, Los Angeles, CA 90089.

[2] Lomonosov Moscow State University, Department of Aeromechanics and Gas Dynamics, School of Mechanics and Mathematics, Moscow 119899, Russia; and Space Research Institute RAS and Institute for Problems in Mechanics RAS; izmod@ipmnet.ru.

[3] Astronautics and Space Technology Division, School of Engineering, University of Southern California, Los Angeles, CA 90089.

TABLE 1

SPACECRAFT POSITION, LOOK DIRECTION, OBSERVED INTENSITY, AND SOLAR FLUX

Spacecraft	Year	Day	Heliocentric Distance (AU)	Spacecraft Latitude[a]	Spacecraft Longitude[b]	Look Direction Latitude[c]	Look Direction Longitude[d]	Intensity (R)	Solar Flux (photons cm^{-2} s^{-1})	GC–Look Direction Angle[e]
V1	1989	279	39.1	32.7	241.1	8.4	260.1	280	5.96E+11	5.6
	1989	279	39.1	32.7	241.1	14.9	267.7	221	5.96E+11	9.8
	1989	279	39.1	32.7	241.1	4.2	250.9	245	5.96E+11	13.9
	1989	279	39.1	32.7	241.1	1.4	282.7	218	5.96E+11	18.2
	1989	279	39.1	32.7	241.1	2.7	241.9	221	5.96E+11	23.9
	1989	279	39.1	32.7	241.1	13.6	292.0	286	5.96E+11	27.9
	1989	279	39.1	32.7	241.1	−17.3	241.1	253	5.96E+11	32.2
	1989	279	39.1	32.7	241.1	−15.0	225.4	269	5.96E+11	44.2
V2	1990	143	32.0	−2.5	281.4	−30.5	270.0	270	5.63E+11	36.32
	1990	143	32.0	−2.5	281.4	−32.5	281.4	276	5.63E+11	41.13
	1990	143	32.0	−2.5	281.4	−30.5	292.8	236	5.63E+11	44.85
	1990	143	32.0	−2.5	281.4	−24.9	302.2	239	5.63E+11	47.28
	1990	143	32.0	−2.5	281.4	−7.2	311.2	232	5.63E+11	47.87
	1990	143	32.0	−2.5	281.4	−16.7	308.3	202	5.63E+11	48.31
	1990	143	32.0	−2.5	281.4	−48.4	258.2	266	5.63E+11	54.19
	1990	143	32.0	−2.5	281.4	6.0	330.7	234	5.63E+11	65.48
	1990	143	32.0	−2.5	281.4	−9.3	331.3	246	5.63E+11	67.76
P10	1981	1	23.40	3.060	60.739	...	...	70.2	5.60E+11	...
	1981	4	23.42	3.057	60.752	...	...	68.9	5.52E+11	...
	1981	7	23.45	3.054	60.765	...	...	67.1	5.45E+11	...
	1981	10	23.47	3.052	60.778	...	...	65.8	5.39E+11	...
	1981	13	23.49	3.052	60.763	...	...	65.3	5.34E+11	...
	1981	16	23.52	3.054	60.735	...	...	67.1	5.34E+11	...
	1981	19	23.55	3.057	60.909	...	...	68.7	5.37E+11	...
	1981	22	23.57	3.060	61.184	...	...	65.4	5.39E+11	...
	1981	25	23.59	3.068	61.162	...	...	70.7	5.41E+11	...
	1981	28	23.61	3.068	61.098	...	...	69.6	5.42E+11	...
	1981	31	23.64	3.063	61.012	...	...	69.3	5.45E+11	...
	1981	34	23.66	3.057	60.926	...	...	67.5	5.47E+11	...
	1981	37	23.68	3.052	60.841	...	...	64.6	5.49E+11	...
	1981	40	23.71	3.054	60.808	...	...	64.2	5.50E+11	...
	1981	43	23.73	3.055	60.775	...	...	65.5	5.53E+11	...
	1981	46	23.75	3.062	60.784	...	...	68.3	5.55E+11	...
	1981	49	23.78	3.069	60.792	...	...	68.6	5.58E+11	...
	1981	52	23.80	3.073	60.795	...	...	67.5	5.62E+11	...
	1981	55	23.83	3.072	60.785	...	...	67.1	5.65E+11	...
	1981	58	23.85	3.071	60.775	...	...	68.1	5.67E+11	...
	1981	61	23.87	3.076	60.780	...	...	68.2	5.69E+11	...

[a] Sun-centered ecliptic latitude of the spacecraft.
[b] Sun-centered ecliptic longitude of the spacecraft.
[c] Sun-centered ecliptic latitude of the look direction; *P10* look direction is described in the text.
[d] Sun-centered ecliptic longitude of the look direction; *P10* look direction is described in the text.
[e] Angle between look direction and Galactic center (GC); angle between *P10* look angle and GC direction is discussed in the text.

Broadfoot et al. (1977, 1981). A detailed description of the *P10* UV photometer is given by Carlson & Judge (1974).

We have used eight *V1* cruise maneuver data points obtained on 1989 day 279 at a heliocentric distance of 39.1 AU. The cruise maneuver observations were designed to gather observations of the Lyα resonance emissions over large portions of the sky and lasted from 4 to 20 hours (Hall 1992). The ecliptic latitude of *V1* was 32.°7, and the ecliptic longitude was 241.°1 during the observations (Table 1). Look directions of the *V1* data points (Table 1) used here sampled regions 5°–44.°2 from the Galactic center. The look directions have been chosen to traverse regions far from the Sun so that optical thickness ensures uniform solar illumination along the line of sight.

We have used nine *V2* cruise maneuver data points obtained on 1990 day 143 at a heliocentric distance of 32.0 AU. The ecliptic latitude of *V2* was −2.°5 and ecliptic longitude was 281.°4 during the observations (Table 1). Look directions of the *V2* data points (Table 1) used, sampled regions 36°–68° from the Galactic center.

We have used 21 *P10* daily averaged Lyα data points obtained in early 1981 at about 23 AU from the Sun. The ecliptic latitude of *P10* was 3.°1 and ecliptic longitude 60° (Table 1). The *P10* photometer look angle traces out a conical shell (apex angle 40° and shell thickness 1°) about the spacecraft spin axis pointing approximately in the direction of the Earth. *P10* was downwind with respect to the interstellar flow and the look directions for all the selected data points sampled the downwind direction approximately 135°–175° from the Galactic center.

The solar Lyα flux values used in the calculation were obtained on the basis of Woods et al. (2000).[4] The solar Lyα intensities

[4] See the Web site http://spacewx.com for Lyα values used.

given in the Web site are mostly actual measurements although *Solar Mesospheric Explorer* measurements have been rescaled to match the SUSIM UARS calibration and the He 10830 Å has been used as a proxy to fill in some gaps. The solar Lyα flux values used here have been obtained by averaging the daily data over a month to take into account the fact that all three spacecraft would see only an average illumination due to their being at large heliocentric distances.

5. COMPARISON OF CALCULATIONS TO OBSERVATIONS

Monte Carlo radiative transfer calculations were carried out for various neutral hydrogen density models. The calculated results for the various neutral density models were then compared with the *P10*, *V1*, and *V2* EUV data. It was necessary to calculate the optimum *P10*, *V1*, and *V2* calibration factors (CFs) for each of the density models because of the well-known calibration differences between the *V1*, *V2*, and *P10* spacecraft detectors at Lyα (Shemansky et al. 1984). The calibration factor for a particular density model is obtained by minimizing the least squares sum (LSS) given by the following equation:

$$\mathrm{LSS} = \sum \left[(I_{\mathrm{model}} - \mathrm{CF} I_{\mathrm{space}})/\sigma \right]^2, \qquad (1)$$

where I_{model} is the calculated intensity, I_{space} is the measured intensity, σ is the standard error for each data point and summation is over the *P10* or *V1* or *V2* data points. We have assumed a zero Galactic Lyα background since, except possibly for the region close to the Galactic center, the Galactic Lyα background has been found to be small (Shemansky et al. 1984; Gangopadhyay et al. 2002, 2005; Quemerais et al. 2003). The standard error σ is given by the following equation:

$$\sigma = I \sqrt{\left(\frac{\delta n}{n}\right)^2 + \left(\frac{\delta F}{F}\right)^2},$$

where I is the calculated intensity, $\delta n/n$ is the fractional uncertainty in the number of photons, n, collected by the detector, and $\delta F/F$ is the fractional uncertainty in the solar flux, F, used here; $\delta n/n$ is given by $1/\sqrt{n}$. The fractional uncertainty in solar flux, estimated from the standard deviation of the daily solar flux during the *V1*, *V2*, and *P10* observations, was found to be about 5% during 1989–1990 (near solar maximum) and about 1% during early 1981 (approaching solar minimum). Thus $\delta F/F$ was set equal to 0.05 for *V1* and *V2* data and equal to 0.01 for *P10* data.

TABLE 2
SETS OF MODEL PARAMETERS AND RESULTS

Spacecraft	H Density (cm^{-3})	Proton Density (cm^{-3})	$(\mathrm{LSS})^{1/2}$	CF
V1	0.15	0.05	2.25	0.56
V1	0.15	0.07	2.53	0.54
V1	0.18	0.06	2.22	0.67
V1	0.2	0.1	2.62	0.69
V2	0.15	0.05	1.25	0.35
V2	0.15	0.07	1.73	0.34
V2	0.18	0.06	1.00	0.43
V2	0.2	0.10	2.99	0.45
P10	0.15	0.05	0.31	2.0
P10	0.15	0.07	0.39	1.76
P10	0.18	0.06	0.41	1.97
P10	0.2	0.10	0.44	2.12

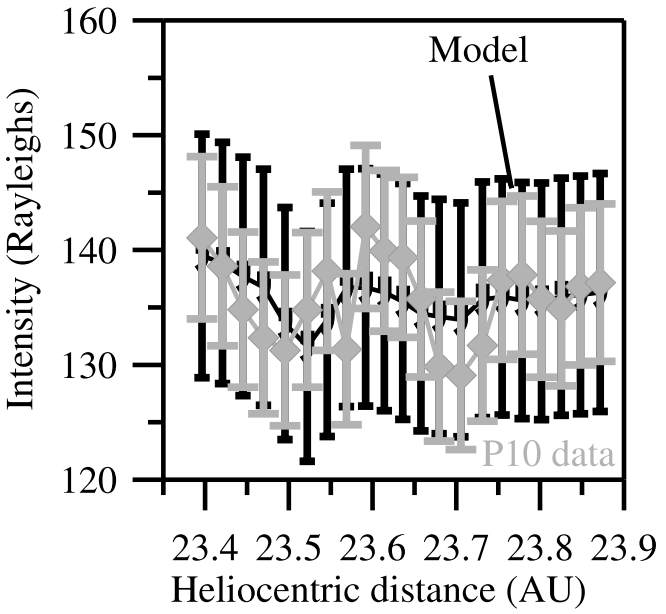

FIG. 1.—Calculated intensity for the heliospheric model with neutral hydrogen density of 0.15 cm^{-3} and proton density of 0.05 cm^{-3} and *P10* intensity modified by a calibration factor of 2.0 are plotted against spacecraft heliocentric distance. The standard error for the calculated intensity in this and subsequent figures is calculated by the equation given in the text. [*See the electronic edition of the Journal for a color version of this figure*.].

The LSS is a measure of the fit of the calculated results with the data of a particular spacecraft, the smaller the LSS better the fit for that spacecraft. The $(\mathrm{LSS})^{1/2}$ and CF for *P10*, for *V2*, and for *V1* are shown in Table 2. It is clear from Table 2 that none of the four VLISM models best fits the data from all three spacecraft. While the heliospheric model with neutral hydrogen density of 0.18 cm^{-3} and proton density of 0.06 cm^{-3} best fits

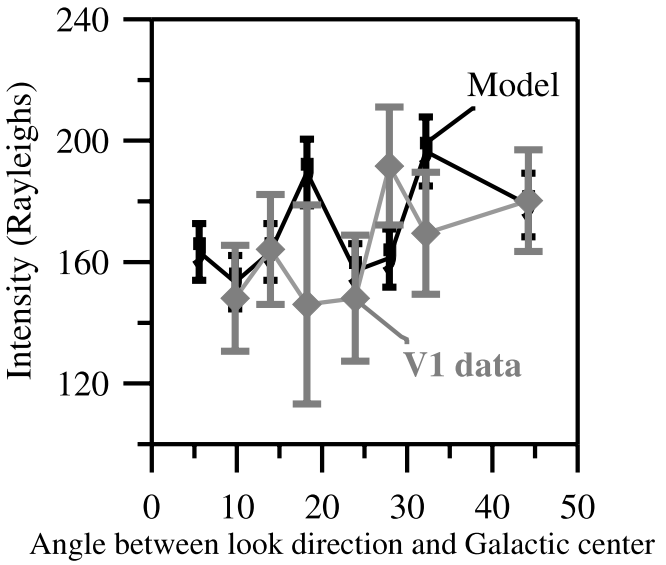

FIG. 2.—Calculated intensity for the heliospheric model with neutral hydrogen density of 0.18 cm^{-3} and proton density of 0.06 cm^{-3} and *V1* intensity modified by a calibration factor of 0.67 are plotted against the angle between the line of sight and the Galactic center. [*See the electronic edition of the Journal for a color version of this figure*.]

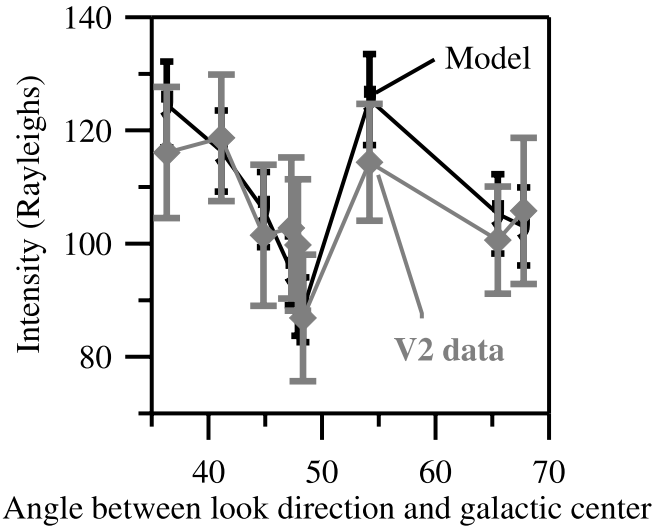

FIG. 3.—Calculated intensity for the heliospheric model with neutral hydrogen density of 0.18 cm^{-3} and proton density of 0.06 cm^{-3} and *V2* intensity modified by a calibration factor of 0.43 are plotted against the angle between the line of sight and the Galactic center. [*See the electronic edition of the Journal for a color version of this figure.*]

both the *V1* data and the *V2* data sets, the *P10* data were best fitted by the heliospheric model with the neutral hydrogen density of 0.15 cm^{-3} and proton density of 0.05 cm^{-3}. The *P10*, *V1*, and *V2* data as modified by the appropriate CF and the calculated intensities are shown in Figures 1, 2, and 3 for the best-fit heliospheric models, respectively.

6. DISCUSSION AND CONCLUSION

What could be the reason or reasons for our failure to find a single heliospheric plasma-neutral model fitting both the downstream and the upstream data? One possibility is simply that we did not choose the right VLISM heliospheric model, since we tested only a few VLISM models with different neutral hydrogen and proton densities. The second possibility is that we are seeing the effect of the squeezing of the heliospheric interface due to the interstellar magnetic field. There is no doubt that magnetic fields affect the heliospheric neutral hydrogen density. A model like that of Izmodenov et al. (2005) that incorporates the interstellar magnetic field and uses a kinetic treatment of the neutral H atom flow should be used in the future for the interpretation of the glow data. The third possibility is that we are seeing time-dependent effects. It is of course certain that a time-dependent heliosphere model will be necessary to fully interpret the glow data because the heliosphere is expected to "breathe in or out" due to pressure fluctuations caused by the well-known solar cycle variations. In this case there will be regions of high neutral hydrogen density followed by regions of lower density, because the amount of VLISM neutral hydrogen filtering through the interface will change over an entire solar cycle and will cause the neutral hydrogen density inside the heliosphere to fluctuate. This fluctuation in neutral hydrogen density would show up as a change in VLISM parameters when a stationary model is used. Another possible time-dependent effect that might show up in the data results because H atoms take most of the solar cycle to drift across the heliosphere, so that while *V1* and *V2* are observing H atoms currently crossing into the supersonic region, the *P10* observation is influenced by previous solar cycle effects imprinted on the downstream neutrals. This might explain why the neutral hydrogen density obtained from *V1* and *V2* observations obtained within 229 days of each other differed from that obtained from *P10* data obtained more than 8 years previously. The modulation of the hydrogen density due to the solar cycle variation of the radiative flux (Blum et al. 1993; Kyrola et al. 1994; Rucinski & Bzowski 1995) will not significantly affect the results presented here since deviations of the glow intensity from the stationary model glow intensity are negligible (less than 3%) (Rucinski & Bzowski 1995) beyond distances $\sim$15 AU from the Sun in the upwind direction and beyond $\sim$30 AU in the downwind direction. The *V1* and *V2* data obtained at distances greater than 30 AU from the Sun in the upwind direction are clearly not affected by the solar cycle effect. The solar cycle effect on the *P10* data obtained when *P10* was situated 15° from the downwind direction and at distances greater than 23 AU from the Sun and along look angles surveying a region between 0° and $\sim$35° from the downwind direction would be small.

The time-dependent and magnetic field effects seen here are in qualitative agreement with the recent *V1* observations (Quemerais et al. 2003). It is not possible to make any quantitative comparison between the time-dependent and magnetic field effects seen by *V1*, *V2*, and *P10* at medium heliocentric distances and the effect seen by *V1* at distances greater than 70 AU since time-independent heliospheric models cannot capture the complexity of the actual neutral hydrogen distribution in the heliosphere. The relatively longer length of the line of sight of the *P10* photometer compared to that of the *V1* and *V2* spectrometers, due to the relatively lower neutral hydrogen density compared to the upstream density, creates difficulty in the interpretation of the combined UV backscattering data set. *V1* and *V2* spectrometer lines of sight in the upwind heliosphere, for example, are only a few tens of AU long compared to the much longer *P10* photometer line of sight since the downwind hydrogen density remains depressed for hundreds of AU relative to the upwind heliosphere. This implies that the *P10* photometer peered deeper into the past than the *V1* and the *V2* spectrometers. This would not matter if the heliosphere is a static body, which we know from the recent *V1* data to be not true. The results presented here suggest the need to use heliospheric models that incorporate both time dependence and magnetic fields. These models are still under development.

Solar Lyα line shape variations may also need to be taken into account. It is well known that photons from the solar Lyα line core and not the wings resonantly scatter from the inflowing interstellar hydrogen atoms. What is measured, however, is the solar flux integrated over the whole line and not the core. The fraction of core photons will vary with the solar cycle if there is any solar cycle line shape variation. We have in this calculation assumed a fixed line shape (Lemaire et al. 1978), which may not hold over the entire solar cycle (Lemaire et al. 1998).

Finally, the result presented here is not a manifestation of the well-known calibration difference between *P10* and *V1* and *V2* at Lyα (Shemansky et al. 1984; Gangopadhyay et al. 2005). This is because heliospheric models with different hydrogen and proton densities will yield backscattered glow with different functional dependencies on look angles and heliocentric distances, and the procedure of minimization of LSS described previously can discriminate between the different functional dependencies and thus the different heliospheric models. The result obtained in this work suggests that the four heliospheric models used here had different functional dependencies on look angles and heliocentric distances, and thus there was no need to know the absolute values of the glow intensities.

We acknowledge with pleasure a very fruitful discussion with H. S. Ogawa. This work was supported by NASA grant NNG04GB80G. It is a pleasure to acknowledge the computational support given by the University of Southern California High Performance Computing and Communication (HPCC) center. V. I. was supported in part by grants RFBR 04-02-16559, RFBR-CNRS (PICS) 05-02-22000, and International Space Science Institute in Bern.

REFERENCES

Axford, W. I. 1972, in Solar Wind, ed. C. P. Sonett, P. J. Coleman, Jr., & J. M. Wilcox (NASA SP-308; Washington: NASA), 609
Baranov, V. B., & Malama, Yu. G. 1993, J. Geophys. Res., 98, 15157
———. 1995, J. Geophys. Res., 100, 14755
Blum, P., Gangopadhyay, P., Ogawa, H. S., & Judge, D. L. 1993, A&A, 272, 549
Broadfoot, A. L., et al. 1977, Space Sci. Rev., 21, 183
———. 1981, J. Geophys. Res., 86, 8259
Carlson, R. W., & Judge, D. L. 1974, J. Geophys. Res., 79, 3623
Fahr, H. J. 2004, Adv. Space Res., 34, 3
Gangopadhyay, P., Izmodenov, V. V., Gruntman, M., & Judge, D. L. 2002, J. Geophys Res., 107, 17
Gangopadhyay, P., Izmodenov, V. V., Quemerais, E., Gruntman, M., & Judge, D. L. 2004, Adv. Space Res., 34, 94
Gangopadhyay, P., Izmodenov, V. V., Shemansky, D E., Gruntman, M., & Judge, D. L. 2005, ApJ, 628, 514
Gangopadhyay, P., Ogawa, H. S., & Judge, D. L. 1989, ApJ, 336, 1012
Hall, D. 1992, Ph.D. thesis, Univ. Arizona
Holzer, T. E. 1972, J. Geophys Res., 77, 5407
Izmodenov, V. V. 2000, Ap&SS, 274, 55
———. 2003, in Interstellar Environment of the Heliosphere, ed. D. Breitschwerdt & G. Haerendel (MPE Report 285; Garching: MPE), 113
———. 2004, in The Sun and the Heliosphere as an Integrated System, ed. G. Poletto & S. T. Suess (Dordrecht: Kluwer), 23
Izmodenov, V. V., Alexashov, D. B., & Myasnikov, A. V. 2005, A&A, 437, L35
Izmodenov, V. V., Gangopadhyay, P., Quemerais, E., Gruntman, M., & Judge, D. L. 2003, in AIP Conf. Proc. 679, Solar Wind Ten, ed. M. Velli, R. Bruno, & F. Malara (Melville: AIP), 198
Izmodenov, V. V., Geiss, J., Lallement, R., Gloeckler, G., Baranov, V. B., & Malama, Yu. G. 1999, J. Geophys Res., 104, 4731
Izmodenov, V. V., Gruntman, M., & Malama, Yu. G. 2001, J. Geophys Res., 106, 10681
Kyrola, E., Summanen, T., & Raback, P. 1994, A&A, 288, 299
Lemaire, P., Charra, J., Jouchox, A., Vidal-Madjar, A., Artzner, G. E., Vial, J. C., Bonnet, R. M., & Skumanich, A. 1978, ApJ, 223, L55
Lemaire, P., Emerich, C., Curdt, W., Schuehle, U., & Wilhelm, K. 1998, A&A, 334, 1095
Malama, Yu. G. 1991, Ap&SS, 176, 21
Quemerais, E., Bertaux, J.-L., Lallement, R., Sandel, B. R., & Izmodenov, V. 2003, J. Geophys. Res., 108, 4
Rucinski, D., & Bzowski, M. 1995, A&A, 296, 248
Shemansky, D. E., Judge, D. L., & Jessen, J. M. 1984, in Local Interstellar Medium (NASA CP-81; Greenbelt: NASA), 24
Woods, T. N., Tobiska, W. K., Rottman, G. J., & Worden, J. R. 2000, J. Geophys. Res., 105, 27195
Zank, G. P. 1999, Space Sci. Rev., 89, 413